Reed valve simulation using 3D high-order finite volume and finite element methods

Pablo Castrillo[1,2], Eugenio SCHILLACI[1,*], Joaquim RIGOLA[1]

[1] Universitat Politècnica de Catalunya - Barcelona Tech (UPC),
ESEIAAT, C/ Colom, 11, 08222, Terrassa (Barcelona), Spain.

[2] Instituto de Estructuras y Transporte, Facultad de Ingeniería, Universidad de la República,
Montevideo, Uruguay.

[*] Corresponding Author (eugenio.schillaci@upc.edu)

ABSTRACT

The shear locking effect occurs in bending-dominant computational solid dynamics problems due to the inability of the element edges to bend, causing the appearance of artificial shear deformation. A common real example where this effect appears is in compressor reed valves. The problem can be solved by using very refined meshes or by employing high-order discretization models. This is straightforward in FEM but not fully mature for FVM models.

In this work, a reed valve problem with impact is solved by means of the high-order FVM structural dynamic solver previously presented by the authors. A new strategy to deal with the impact between the valve and the solid seat is presented. Results are verified by comparison to a past experimental work and compared to those obtained by a structural FEM solver, demonstrating the reliability of this new FVM-CSD methodology.

1. INTRODUCTION

Since its most original formulations, the Finite Volume Method (FVM) is usually associated with fluid and heat transfer problems. Unlike other numerical methods, such as the Finite Element Method (FEM) and the Finite Difference Method, which were first devised to solve problems in solid mechanics, the FVM began to be used in this field only in the last few years. FVM has always excelled in Computational Fluid Dynamics (CFD) by solving equations that come from conservative laws; it has a straightforward mathematical formulation, and fluxes only need to be evaluated on the faces of the elements, making the method simpler and cheaper from a computational point of view. On the other hand, and unlike FVM methods, FEM has always stood out for its ability to increase, in a straightforward way, the order of interpolation of the main variable of the problem. This is an advantage for Computational Solid Dynamics (CSD) problems, especially when stress concentration problems or the shear locking effect appear.

The shear locking occurs in bending-dominant problems due to the inability of the element edges to bend, which causes the appearance of artificial shear deformation, making the element stiffer. This problem happens when using FEM or FVM with linear interpolation. Refining the mesh may solve the problem, however, with usually unacceptable computational costs. The best way to address the problem is to increase the interpolation order. A common real example where the effect of shear locking appears is in compressor reed valves, due to their small thickness. Their simulation is of great industrial interest since it would allow predicting the failure of the piece, usually caused by fatigue. This problem was traditionally addressed by means of FEM models, but recently, a fully 3D high-order FVM model for solid mechanics was presented by the authors to solve shear dominant problems, opening the way to fully couple Fluid-Structure Interaction simulations with a common finite volume discretization framework for both turbulent fluid dynamics and solid mechanics (Castrillo, Schillaci, & Rigola, 2024). The current paper wants to address a particular necessity: showing how FVM-CFD and FEM-CFD models can give comparable and reliable results in the resolution of a reed valve problem affected by the shear locking effect.

The test case is a simulation of a compressor reed valve subjected to a pulsating air flow, considering the

interaction between fluid and structure and the impact of the valve on the seat, replicating an analogous laboratory experiment, employed for validation. A sketch of the experiment is reported in Figure 1 (left). In the experiment, the valve opening is monitored by means of laser measurements and employed for model validation in terms of valve opening and velocity. The laser position is indicated in Figure 1(right). All the experiment details are reported in (Tofique, Löf, Schillaci, Castrillo, & Rigola, 2021).

As advanced, the mentioned problem is solved by using different numerical models: previously, an FSI-CFD model (Tofique et al., 2021) was employed to obtain fluid field and pressure on the valve. In the present work, the fluid pressure on valve surfaces obtained from FSI-CFD simulation is used as input data for FEM-CSD and FVM-CSD simulations. The high-order FVM-CSD method presented in past works (Castrillo, Canelas, Schillaci, Rigola, & Oliva, 2022; Castrillo et al., 2024) is used to obtain displacement, velocity, and stress tensor of the reed valve. This work focuses on the deep analysis of the results and on their comparison with those obtained when using FEM-CSD to solve the same problem.

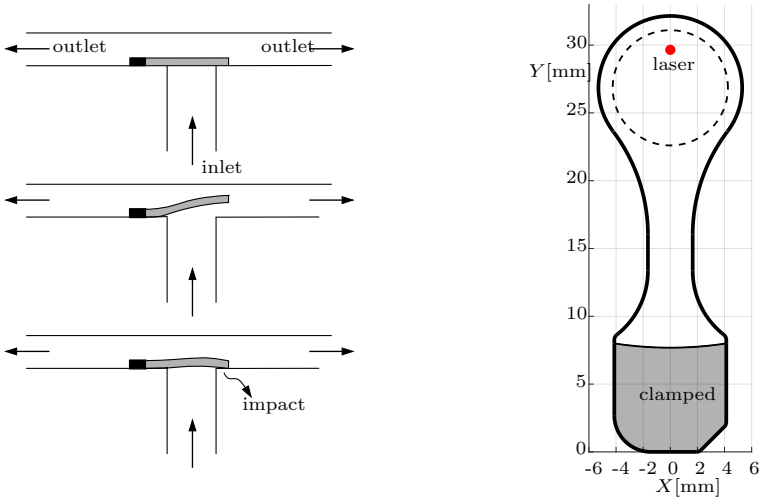

Figure 1: Reed valve problem analyzed in current work: opening and impact of the valve (left), and geometry of the valve (right).

2. NUMERICAL MODELS

This section presents the numerical models used to carry out this work. In previous works (Castrillo et al., 2024), algorithms are presented that can serve as a reference for the reader. Additional details, e.g. algorithm employed for the impact force, are presented in Castrillo's doctoral thesis (Castrillo, 2023).

2.1 Fluid Structure Interaction - Computational Fluid Dynamics (FSI-CFD) Model

The FSI simulation consists of a complex combination of different numerical techniques representing the interaction between a fluid (compressed air) and a solid (reed valve). In particular, the method is characterized by the following items: (1) gas resolution through a finite volume solver on a moving and unstructured mesh; (2) solving the movement of the solid using a 2D simplified plate model; (3) resolution of the fluid-structure interaction through a semi-implicit approach for strongly coupled problems. The entire numerical method is implemented within the Termofluids code (*Termo fluids s.l., www.termofluids.com*, 2020). The fluid-structure coupled problem is solved numerically by a partitioned algorithm using independent solvers for fluid and structural sub-problems and adopting a coupling scheme to account for their interaction. This numerical model, together with simulation results for the reed valve case and their experimental validation, are presented in detail in a previous work (Tofique et al., 2021).

2.2 Finite Element Method - Computational Solid Dynamics (FEM-CSD) Model

As already introduced in (Castrillo, Schillaci, & Rigola, 2021), the pressure applied by the fluid on the valve obtained with the simulation carried out in TermoFluids is used as an input parameter for the FEM-CSD model. Therefore, this external pressure field is used to obtain the valve displacement again (for verification purposes) and to obtain additional insight regarding internal stresses. Differently from (Castrillo et al., 2021),

a new impact model based on (Armero & Petocz, 1998) is introduced in the FreeFEM code to improve the evaluation of impact forces on the valve surface. For the time discretization, the HHT-α method is used, where the parameters of the generalized algorithm, see (Modak & Sotelino, 2002), are $\theta_1 = \theta_2 = \theta_3 = 0.51$, $\gamma_0 = \beta_0 = 3.33015$, $\gamma_1 = \beta_1 = 1.98$, $\gamma_2 = 1/0.51$ and $\beta_2 = 1$. Figure 2 describes the zone of the valve surface on which the contact pressure can be applied. In the formulation presented in (Armero & Petocz, 1998) the function g called *gap* is defined as:

$$g = u_z - 0 = u_z \,, \tag{1}$$

where it is taken into account that the coordinate Z is equal to 0 at the base of the valve (Eq. (1) is particular for this case, the general equation can be found in (Armero & Petocz, 1998)). In Armero's model two parameters are defined to obtain the contact force: (1) the contact parameter k_{imp} is determined for the problem, and, as in (Castrillo et al., 2021), different values of k_{imp} were considered; (2) and, in this work, the parameter ϑ_{imp} is set equal to 1. The impact force $\mathbf{F}_{\text{imp}}$ is obtained as:

$$\mathbf{F}_{\text{imp}} = \int_{A_{\text{imp}}} p_{\text{imp}} \, \mathrm{d}A \, \mathbf{e}_z \,, \tag{2}$$

where p_{imp} is the impact pressure applied in FreeFEM (Hecht, 2012) with the corresponding variational formulation.

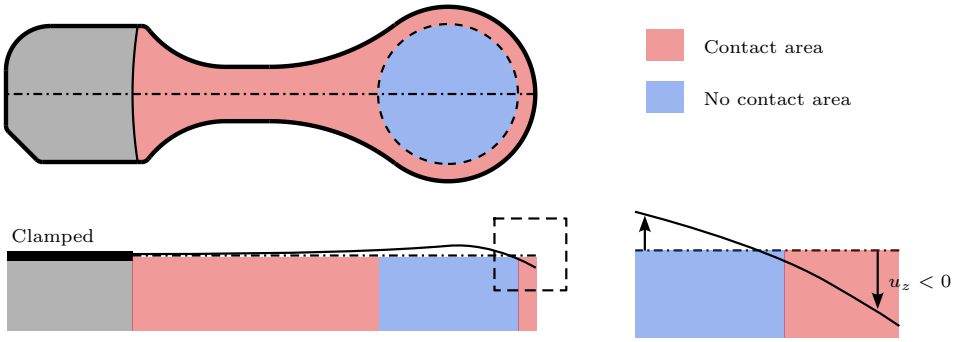

Figure 2: Contact zone used to obtain the impact pressure with the formulation presented in Armero et al. (Armero & Petocz, 1998).

Spatial convergence test To observe the spatial convergence, different meshes have been tested using FreeFEM with quadratic interpolation (p_2). The mesh refinement has been done in two ways: in the plane (left image of Figure 3) and in thickness (right image of Figure 3, where k_{tk} represents the number of refinement lines in that direction). Figure 4 shows the displacement obtained at the point located on the laser. It is possible to observe that spatial convergence is achieved by refining the mesh in both directions. The relative error between the finest and coarse mesh using $k_{\text{kt}} = 1$, where the number of tetrahedrons is increased by 4872, is 0.52 %, while when comparing the finer meshes using $k_{\text{kt}} = 1$ and $k_{\text{kt}} = 4$, where the number of tetrahedrons is increased by 21015, the relative error is 0.08 %. Due to the above, and in order to reduce the computational cost, it is decided to use the finest mesh for $k_{\text{kt}} = 1$.

2.3 Finite Volume Method - Computational Solid Dynamics (FVM-CSD) Model

In this section, the FVM high-order method presented by the authors for 2D (Castrillo et al., 2022) and 3D domains (Castrillo et al., 2024) is used to obtain comparable results to those presented in the previous section. The mesh and the time discretization used are the same as those presented in Section 2.2. In this case the contact force is approximated using $N_{\text{imp}} = 19$ Gauss points as:

$$\mathbf{F}_{\text{imp}}(\mathbf{X}_p) = \int_{A_{\text{imp}}} p_{\text{imp}} \, \mathbf{e}_z \, \mathrm{d}A \approx \sum_{p=1}^{p=N_{\text{imp}}} \alpha_p \, p_{\text{imp}}(\mathbf{X}_p) \, \mathbf{e}_z \,, \tag{3}$$

where α_p and $\mathbf{X}_p$ are the quadrature weights and the coordinates of the p-th Gauss point, respectively. The force $\mathbf{F}_{\text{imp}}$ is imposed as a Neumann condition. For the high-order method (Castrillo et al., 2024), a cubic interpolation with the Local Regression Estimators (LRE) method is used.

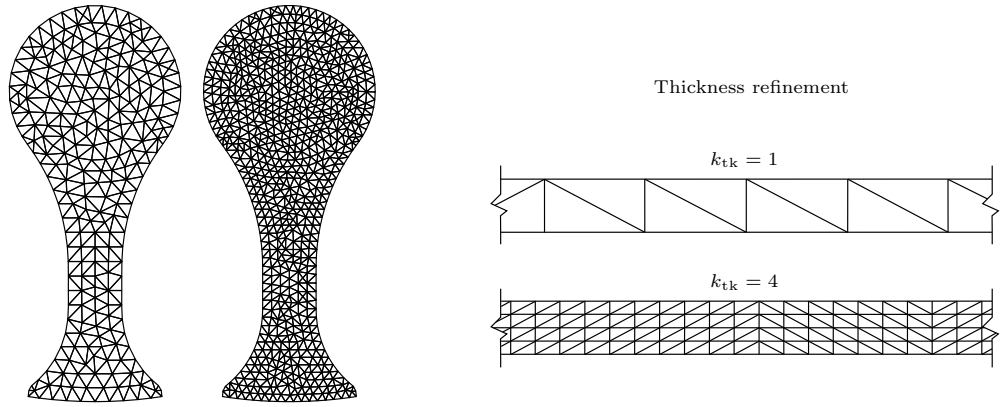

Figure 3: Mesh refinement has been done in two ways: in the plane (left image) and in thickness (right image, where k_{tk} represents the amount of refinement lines in that direction).

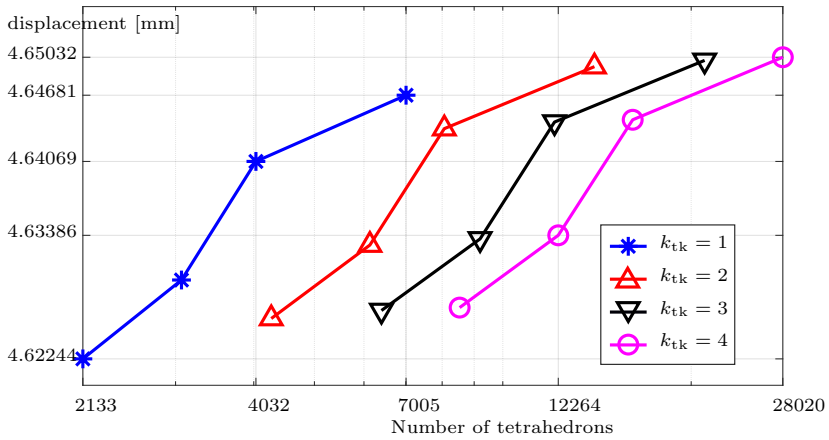

Figure 4: Convergence for different meshes of the displacement at the experimental measurement position.

2.4 Calibration and comparison between FEM and FVM for different k_{imp}

Figure 5 compares, for different values of k_{imp}, the results obtained using FEM with those obtained with the high-order FVM. It is observed that the differences are minimal throughout the valve work cycle. Figure 6 shows the comparison between the results obtained with the TermoFluids simulation, the high order method (for $k_{imp} = 5000\,\text{kPa/mm}$) and the values obtained experimentally. The left image shows the valve displacement, and the right image shows the velocity. It is possible to conclude that, as with TermoFluids, it is possible to capture the velocity peaks. A difference that can be seen with the three-dimensional models of the valve is that the opening of the valve after the second impact occurs a few moments later than in the TermoFluids model. This is explained because in TermoFluids the impacts are practically instantaneous (2-4 instants), while in three-dimensional models, these impacts take several instants, thus prolonging the opening of the valve. Once completed the calibration of the numerical parameter, the model is employed to obtain detailed insights regarding impact forces on valve surfaces and its internal stresses. The results are reported in the next section, where impact forces and pressure are analyzed and compared with that obtained with the high-order method presented in (Castrillo et al., 2024).

3. DETAILED IMPACT ANALYSIS: FVM VS FEM

In this section, the results obtained with the FVM-CSD method regarding the impact force and pressure are reported in detail and compared with those obtained previously with FEM-CSD.

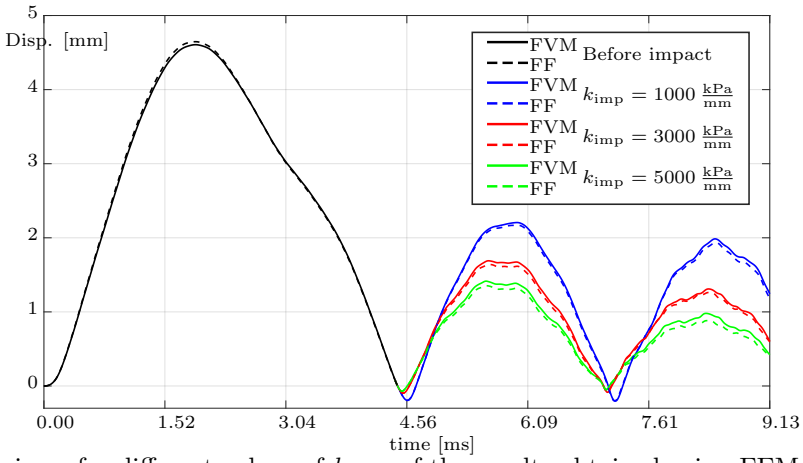

Figure 5: Comparison, for different values of k_{imp}, of the results obtained using FEM and the high-order FVM.

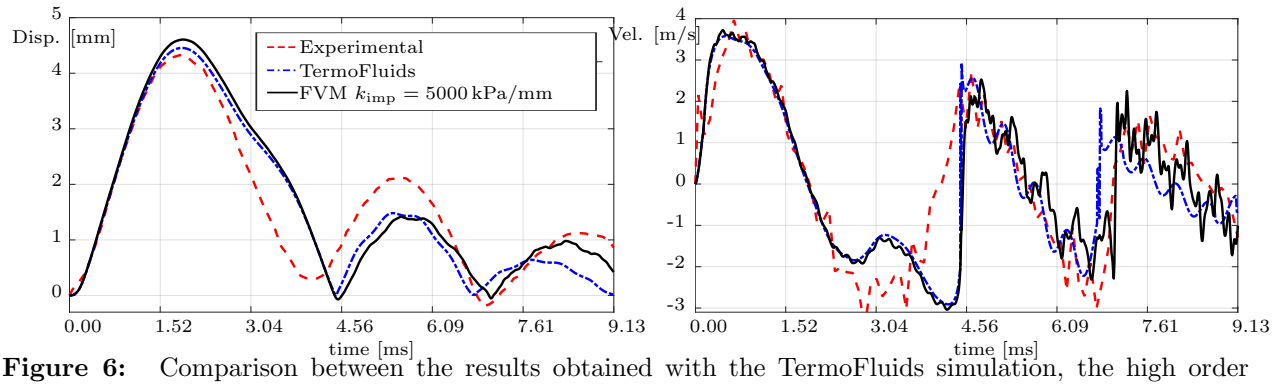

Figure 6: Comparison between the results obtained with the TermoFluids simulation, the high order method (for $k_{\text{imp}} = 5000\,\text{kPa/mm}$), and the values obtained experimentally: valve displacement (left) and valve velocity (right).

3.1 First impact

The first impact occurs during the time interval $T_{\text{FI}} = [4.44, 4.58]$ ms. Figure 7 shows the total impact force and the maximum impact pressure obtained on the valve for the first impact. Both magnitudes grow to a maximum value in this impact and then fall and disappear. It is possible to observe that the solution obtained with both methods are very similar. Figures 8 and 9 show the zone that is in contact with the first impact when using FVM or FEM, respectively. It can be seen that there are practically no differences between the methods. The differences that appear in the images in the second row of each figure are negligible pressure differences and, being close to the neck, have little effect on the behavior of the valve. Figures 10 and 11 show the distribution of the impact pressure on the surface $Z = 0$ for each of the instants of the interval T_{FI} using FVM or FEM, respectively. This impact can be sequenced as: (1) impact begins at the tip of the valve; (2) then the impact pressure is distributed over the valve surface; and (3) finally, the valve is released from the seat. As previously mentioned, the pressure differences near the valve neck in the images of the second row of each figure are negligible.

3.2 Second impact

Regarding the second impact, some differences between the methods are appreciated. The first difference can be seen in Figure 12, where the time interval of the second impact is different for each method. The second impact, when using FEM, starts a few moments earlier with its time interval being $T_{\text{SI, FEM}} = [6.92, 7.13]$, whereas when using FVM, it is $T_{\text{SI, FVM}} = [6.96, 7.12]$. The most significant difference can be seen in the total impact force in the left image of Figure 12. It is observed that in the first part of the second impact (up to an instant $t_1 \approx 7.03$ ms), the force obtained with FVM is greater than with FEM, then both the force and the impact pressure are very similar between the two methods. For both methods, the two magnitudes

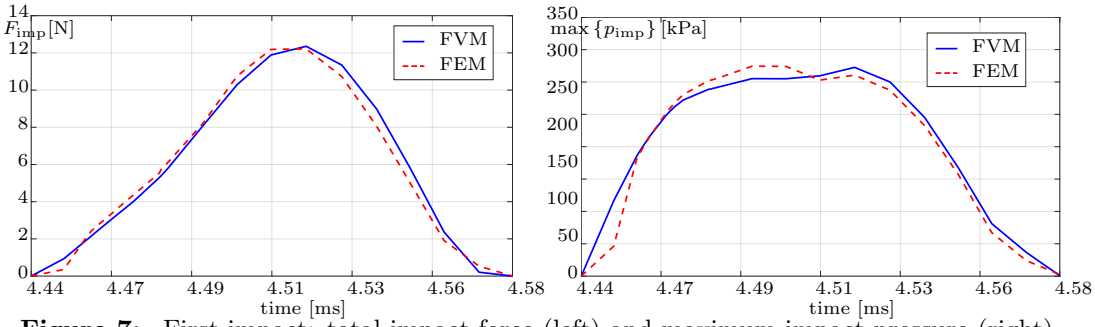

Figure 7: First impact: total impact force (left) and maximum impact pressure (right).

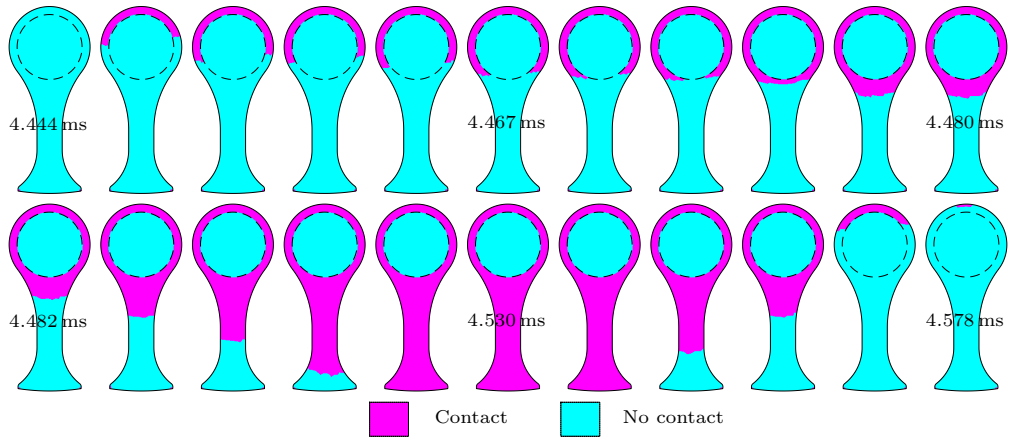

Figure 8: Area of the first impact using FVM.

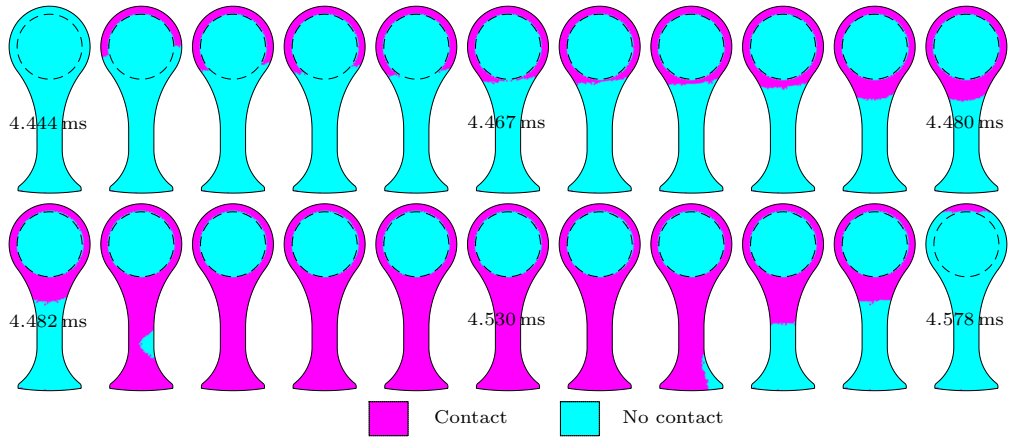

Figure 9: Area of the first impact using FEM.

grow to their maximum value and then fall, rise again, and fall until they disappear. Figure 13 shows the first part of the second impact. It is observed that in the case of FVM, the impact begins between the fluid inlet orifice and the neck of the valve, while in the case of using FEM, the impact begins at the clamped edge and then goes toward the valve. The differences are close to the clamped edge; therefore, it does not create too much distortion between the two solutions in what remains of the process in terms of force and pressure amplitudes, as highlighted in the second part of the impact shown in Figure 12. These differences can be associated with the different interpolations used in each method (quadratic in FEM and cubic in FVM). One method may identify penetration at a different point than the other at the same instant. The important is that the general behavior of this first period of the second impact is similar because a stress

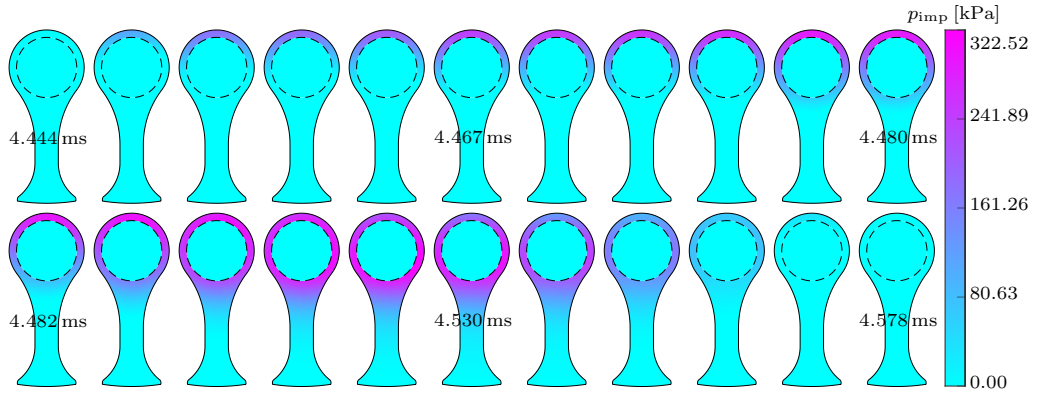

Figure 10: Distribution of the impact pressure in the first impact using FVM.

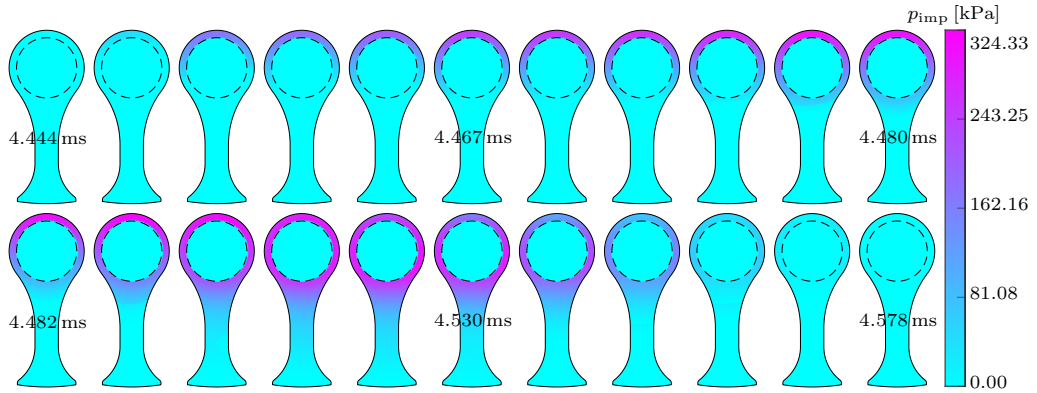

Figure 11: Distribution of the impact pressure in the first impact using FEM.

concentration is generated near the fluid orifice for both methods (the growth, fall, and maximum values occur at the same instants for both methods). In general, this difference does not affect the behavior of the valve along its whole cycle, as previously seen in Figure 5. Figures 14 and 15 show the areas where the second impact occurs when using FVM or FEM, respectively. In these images, the behavior mentioned above is observed. As previously mentioned in the first instants, there are differences in the contact between the methods; see images of the first row of each figure. However, in the second row, the behavior is practically the same, considering that the pressures near the clamped edge in Figure 15 do not affect the behavior of the valve.

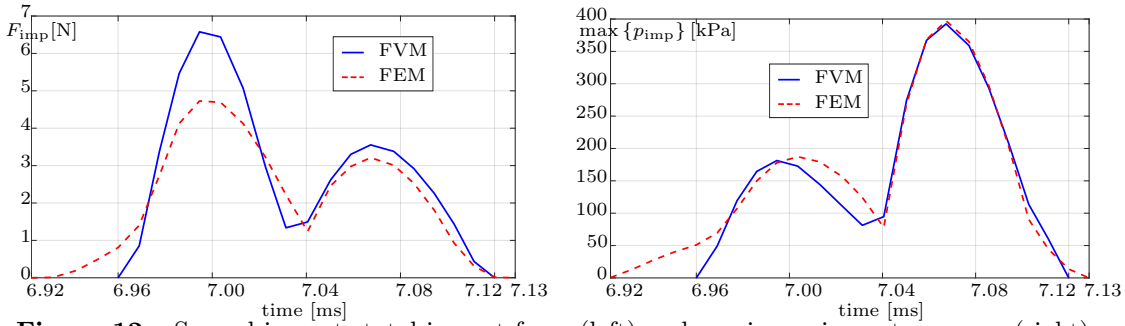

Figure 12: Second impact: total impact force (left) and maximum impact pressure (right).

Figures 16 and 17 show the distribution of the impact pressure on the surface $Z = 0$ for each of the instants of the interval T_{SI} when using FVM or FEM, respectively. This impact can be sequenced as: (1) impact begins between the clamped edge and the inlet fluid orifice spreading towards the tip of the valve; (2) the pressure drops and the impact is again at the tip but on a smaller surface; and (3) finally the valve is released from the seat. It is worth mentioning that a higher maximum pressure is obtained in the second impact

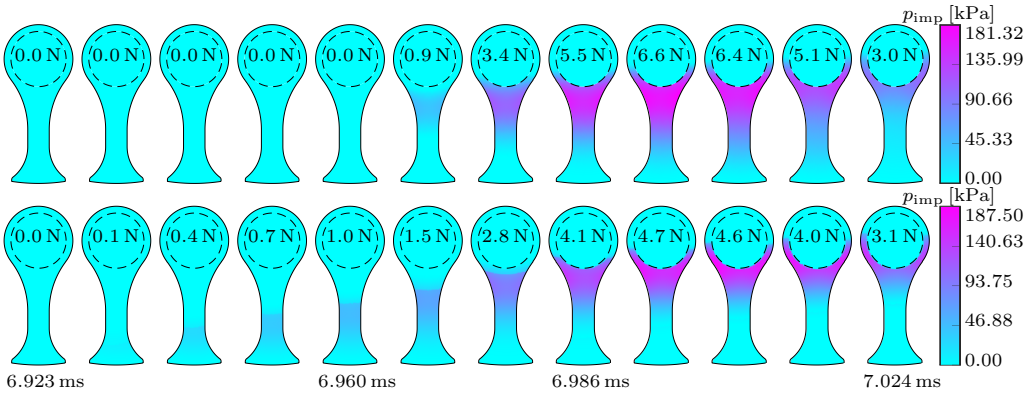

Figure 13: Impact pressure and impact force for the first instants of the second impact using FVM (top images) and FEM (bottom images).

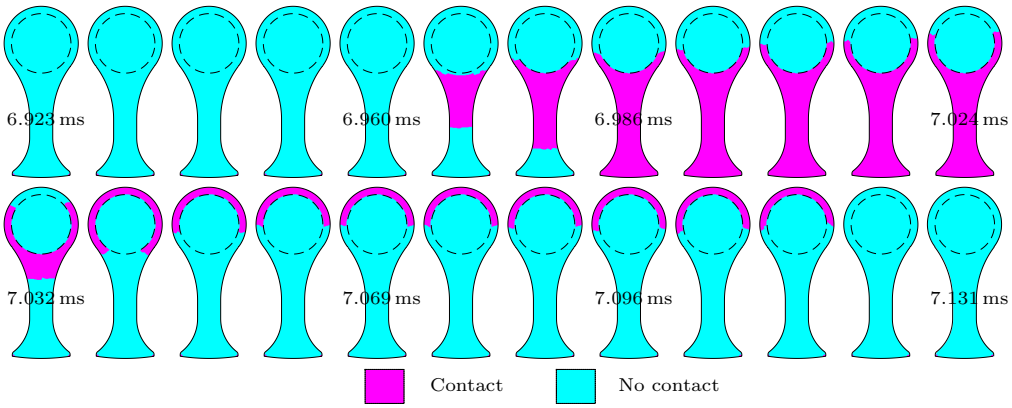

Figure 14: Area of the second impact using FVM.

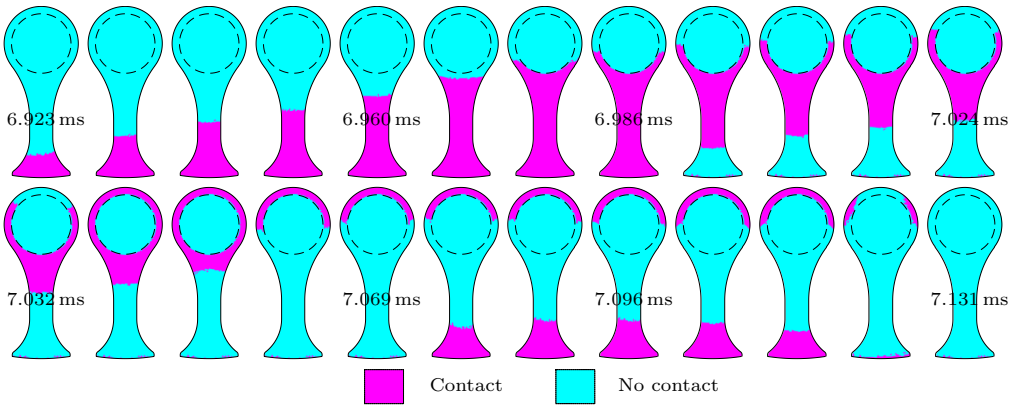

Figure 15: Area of the second impact using FEM.

compared to the first one. This is explained because, despite having lower impact forces, the impact area is smaller, leading to overall greater impact pressures.

3.3 Impact stresses at critical points

As previously discussed, the impact of the valve on the seat is often the cause of valve failure due to fatigue. Figure 18 shows failed reed valves in impact fatigue experiments (Tofique et al., 2021). Some points of the tip of the valve are analyzed to observe the evolution of some stresses. The points to be studied are illustrated in the left image of Figure 19. The stresses analyzed are the maximum and minimum principal

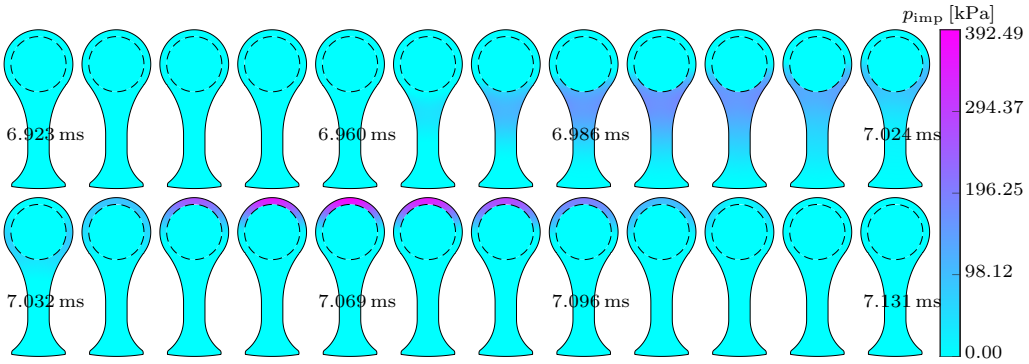

Figure 16: Distribution of the impact pressure in the second impact using FVM.

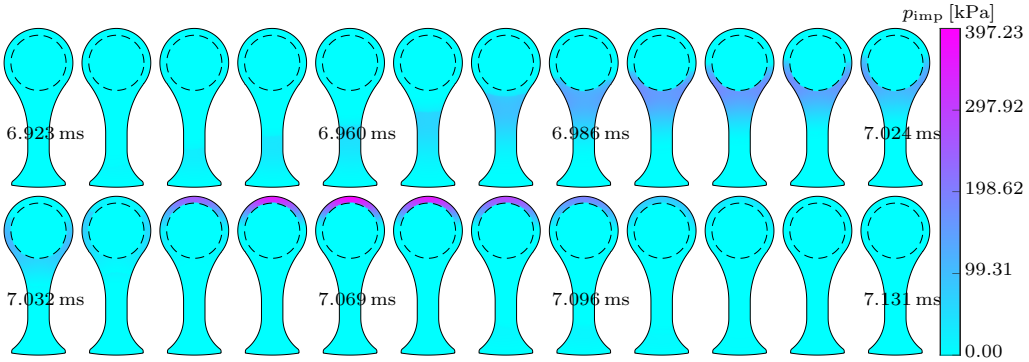

Figure 17: Distribution of the impact pressure in the second impact using FEM.

stress, σ_I and σ_{III}, respectively, and the von Mises stress, commonly used to limit the elastic behavior of ductile materials (especially steels). In the right image of Figure 19 it is observed that the von Mises stress increases for all points in each impact. In those points that are practically not affected by bending (1,2, and 3), a high increase in tensions is noted. Likewise, point 4, which suffers a little from bending, increases stresses due to the impact. Similar results are obtained in Figure 20 for the maximum and minimum principal stresses. Therefore, it is possible to conclude that the numerical simulation shows that the impact generates an important change in the stresses at the points where failures are experimentally observed.

Figure 18: Reed valves in impact fatigue experiments. Taken from (Tofique et al., 2021).

4. CONCLUSIONS

This work analyzes the problem of a reed valve subjected to real working conditions using different computational methods. Two structural codes (FEM-CSD and FVM-CFD) have been employed to obtain detailed insights regarding the internal stresses of a reed valve. A detailed quantitative analysis of the time evolution along a valve cycle of forces and pressure distribution associated with the impacts suffered by the valve against its seat has been proposed. The presented FVM-CSD method provides close results to the universally accepted FEM strategy regarding forces and pressure distribution. From a physical point-of-view, it has been shown that the points indicated as critical and particularly susceptible to rupture from experimental observations suffer a considerable increase in stress due to the impact of the valve.

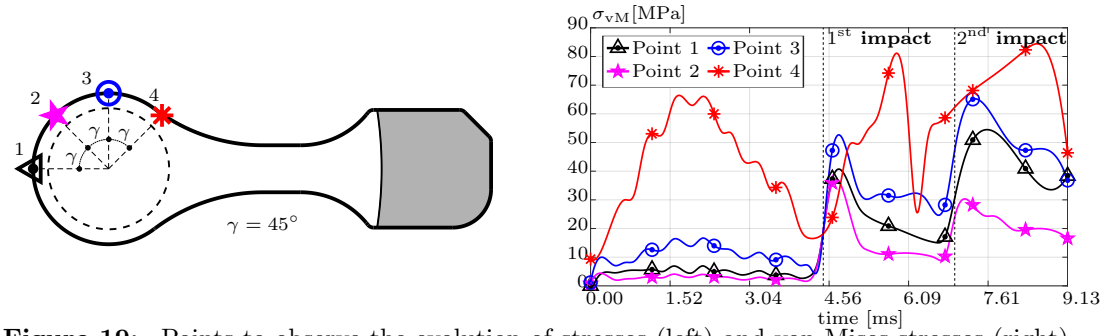

Figure 19: Points to observe the evolution of stresses (left) and von Mises stresses (right).

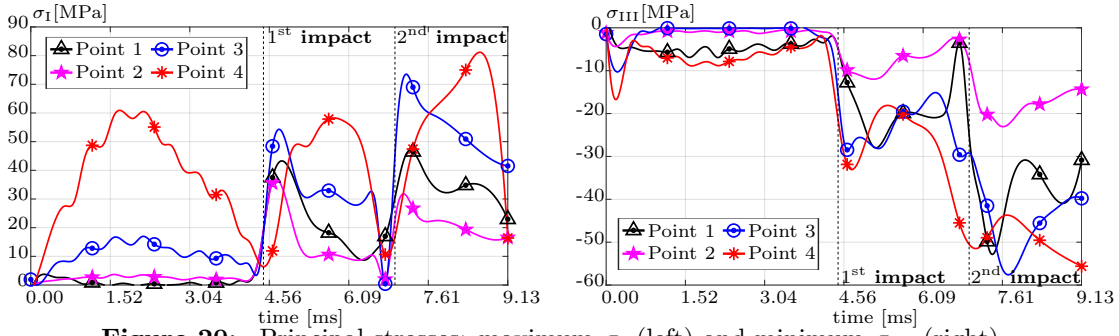

Figure 20: Principal stresses: maximum σ_{I} (left) and minimum σ_{III} (right).

REFERENCES

Armero, F., & Petocz, E. (1998). Formulation and analysis of conserving algorithms for frictionless dynamic contact/impact problems. *Computer Methods in Applied Mechanics and Engineering*, *158*(3-4), 269–300. doi: 10.1016/S0045-7825(97)00256-9

Castrillo, P. (2023). *High-order finite volume method for solid dynamics in fluid-structure interaction applications* (PhD thesis). Universitat Politècnica de Catalunya, Barcelona, Catalunya, Spain. (Available at `https://www.tdx.cat/handle/10803/689330#page=1`)

Castrillo, P., Canelas, A., Schillaci, E., Rigola, J., & Oliva, A. (2022). High-order finite volume method for linear elasticity on unstructured meshes. *Computers & Structures*, *268*, 106829. doi: 10.1016/J.COMPSTRUC.2022.106829

Castrillo, P., Schillaci, E., & Rigola, J. (2021, mar). Simulation of Fluid-Structure Interaction and Impact Force on a Reed Valve. In *14th wccm-eccomas congress 2020* (Vol. 1500, pp. 1–12). Scipedia S.L. Retrieved from `https://www.scipedia.com/public/Castrillo_et_al_2021a` doi: 10.23967/WCCM-ECCOMAS.2020.305

Castrillo, P., Schillaci, E., & Rigola, J. (2024). High-order cell-centered finite volume method for solid dynamics on unstructured meshes. *Computers & Structures*, *295*, 107288.

Hecht, F. (2012). New development in freefem++. *J. of Numerical Math.*, *20*(3-4), 251–265. Retrieved from `https://freefem.org/` doi: 10.1515/jnum-2012-0013

Modak, S., & Sotelino, E. D. (2002, jul). The generalized method for structural dynamics applications. *Advances in Engineering Software*, *33*(7-10), 565–575. doi: 10.1016/S0965-9978(02)00079-0

Termo fluids s.l., www.termofluids.com. (2020). Termo fluids s.l. Retrieved from `www.termofluids.com`

Tofique, M., Löf, A., Schillaci, E., Castrillo, P., & Rigola, J. (2021, may). Experimental and Numerical Analysis Of Reed Valve Movement In An Impact Fatigue Test System and Reciprocating Compressors. In *International compressor engineering conference.* Retrieved from `https://docs.lib.purdue.edu/icec/2697`

ACKNOWLEDGMENT

P. Castrillo gratefully acknowledges the Universitat Politècnica de Catalunya and Banco Santander for the financial support of his predoctoral grant FPI-UPC (109 FPI-UPC 2018).